

## Supporting Information

### **Volatile microemulsion method of preparing water-dispersible photo absorbers for 3D printing of high resolution, high water-content hydrogel structures**

Xiangnan He<sup>ab</sup>, Jianxiang Cheng<sup>ab</sup>, Zechu Sun<sup>ab</sup>, Haitao Ye<sup>ab</sup>, Qingjiang Liu<sup>ab</sup>, Biao Zhang<sup>c\*</sup>, Qi Ge<sup>ab\*</sup>

a. Shenzhen Key Laboratory of Soft Mechanics & Smart Manufacturing, Southern University of Science and Technology, Shenzhen, 518055, China.

b. Department of Mechanical and Energy Engineering, Southern University of Science and Technology, Shenzhen, 518055, China.

c. Research & Development Institute of Northwestern Polytechnical University in Shenzhen, Frontiers Science Center for Flexible Electronics (FSCFE), Xi'an Institute of Flexible Electronics (IFE), Northwestern Polytechnical University, 127 West Youyi Road, Xi'an 710072, China.

\* Email: iambzhang@nwpu.edu.cn, geq@sustech.edu.cn.

†Electronic Supplementary Information (ESI) available.

See DOI: 10.1039/x0xx00000x

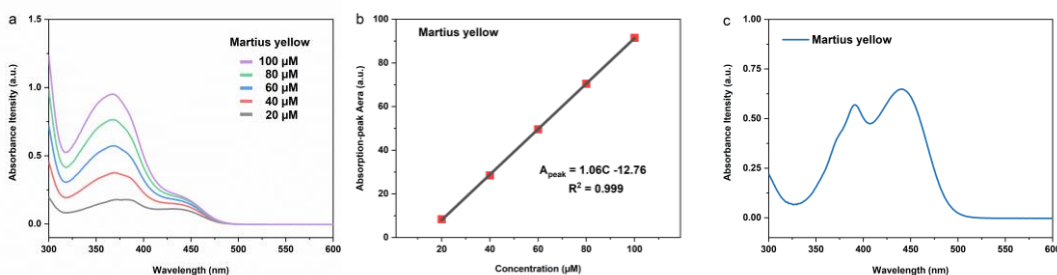


Figure S1. (a) UV-vis spectra of different concentrations of Martius yellow dissolved in ethanol. (b) Plot of absorption-peak area vs. Martius yellow concentration. (c) UV-vis spectra of an ethanol dispersion of 0.5 mg/mL Martius yellow nanoparticles ( $W_{\text{PA}} = 1.7 \text{ wt.}\%$ ).

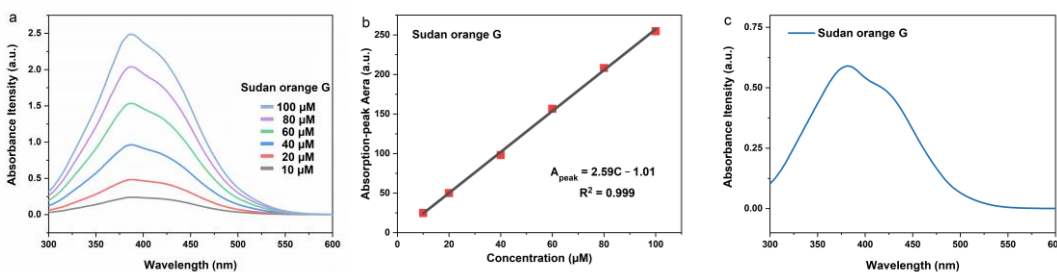


Figure S2. (a) UV-vis spectra of different concentrations of Sudan Orange G dissolved in ethanol. (b) Plot of absorption-peak area vs. Sudan Orange G concentration. (c) UV-vis spectra of an ethanol dispersion of 0.1 mg/mL Sudan Orange G nanoparticles ( $W_{\text{PA}} = 1.7 \text{ wt.}\%$ ).

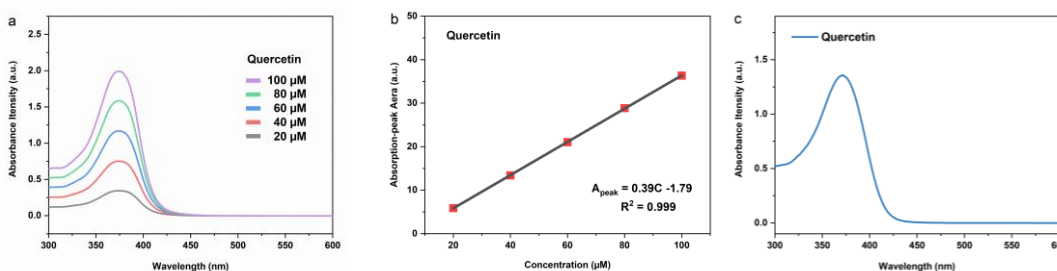


Figure S3. (a) UV-vis spectra of different concentrations of Quercetin dissolved in ethanol. (b) Plot of absorption-peak area vs. Quercetin concentration. (c) UV-vis spectra of an ethanol dispersion of 0.2 mg/mL Quercetin nanoparticles ( $W_{\text{PA}} = 1.7 \text{ wt.}\%$ ).

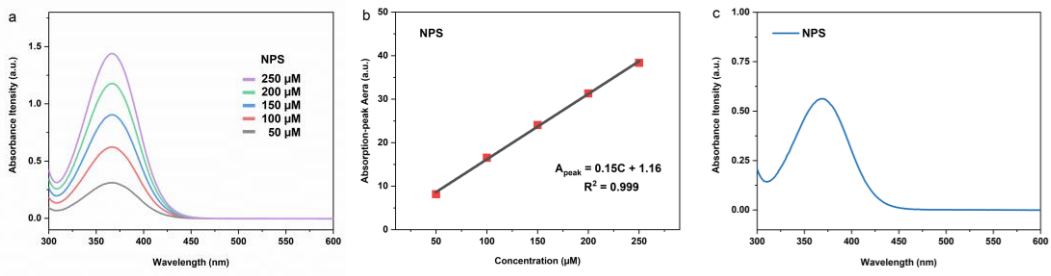


Figure S4. (a) UV-vis spectra of different concentrations of NPS dissolved in ethanol. (b) Plot of absorption-peak area vs. NPS concentration. (c) UV-vis spectra of an ethanol dispersion of 1 mg/mL NPS nanoparticles ( $W_{PA} = 1.7$  wt.%).

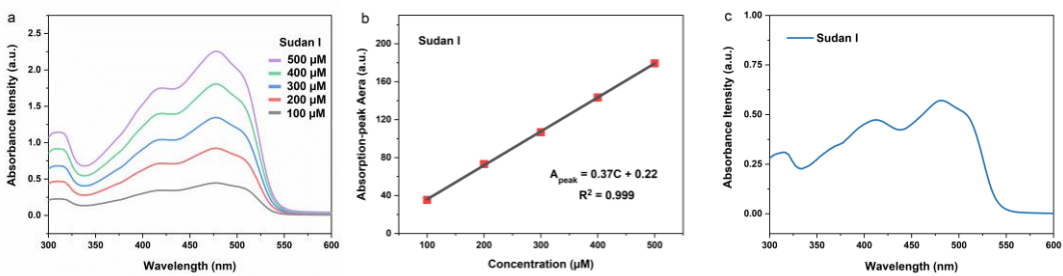


Figure S5. (a) UV-vis spectra of different concentrations of Sudan I dissolved in ethanol. (b) Plot of absorption-peak area vs. Sudan I concentration. (c) UV-vis spectra of an ethanol dispersion of 1 mg/mL Sudan I nanoparticles ( $W_{PA} = 1.7$  wt.%).

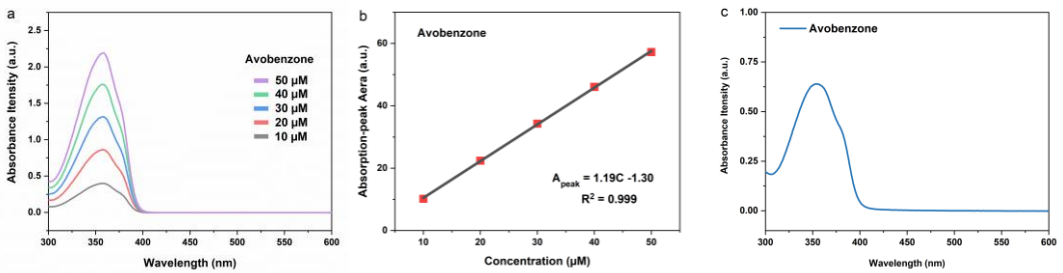


Figure S6. (a) UV-vis spectra of different concentrations of Avobenzone dissolved in ethanol. (b) Plot of absorption-peak area vs. Avobenzone concentration. (c) UV-vis spectra of an ethanol dispersion of 0.2 mg/mL Avobenzone nanoparticles ( $W_{PA} = 1.7$  wt.%).

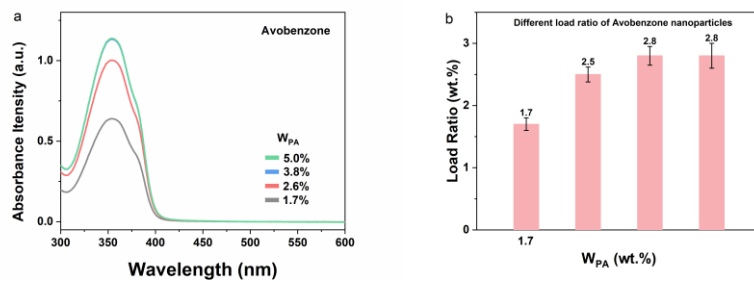


Figure S7. (a) UV-vis spectra of an ethanol dispersion of 1 mg/mL Avobenzone nanoparticles ( $W_{PA}$  from 0.8 wt.% to 5 wt.%). (b) Plot of Avobenzone load ratio in nanoparticles vs. the  $W_{PA}$  of Avobenzone.

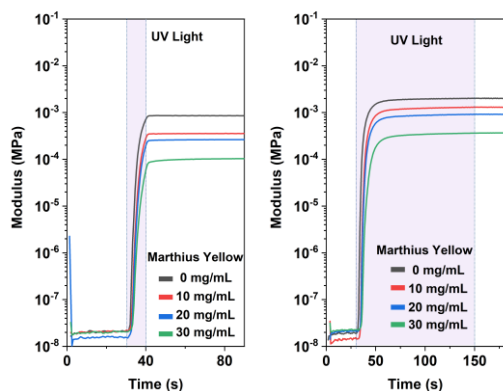


Figure S8. Photorheology curves of hydrogel with Martius Yellow nanoparticles (0 - 30 mg/mL) during short (10 s) and long (120 s) duration light exposures (purple shaded region).

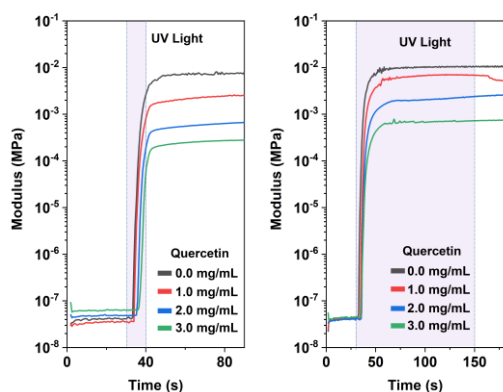


Figure S9. Photorheology curves of hydrogel with Quercetin nanoparticles (0 - 3 mg/mL) during short (10 s) and long (120 s) duration light exposures (purple shaded region).

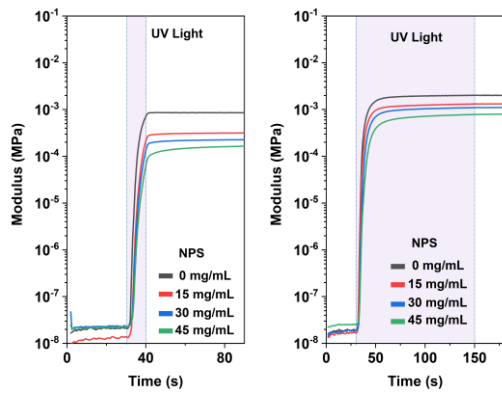


Figure S10. Photorheology curves of hydrogel with NPS nanoparticles (0 - 45 mg/mL) during short (10 s) and long (120 s) duration light exposures (purple shaded region).

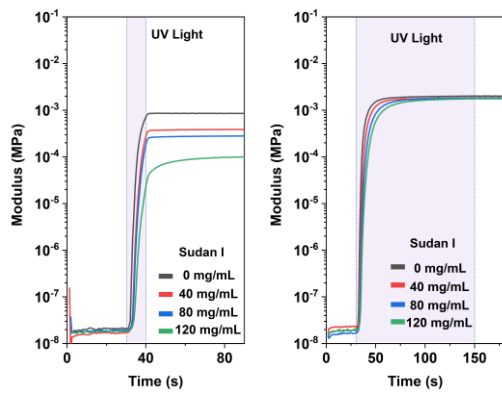


Figure S11. Photorheology curves of hydrogel with Sudan I nanoparticles (0 - 120 mg/mL) during short (10 s) and long (120 s) duration light exposures (purple shaded region).

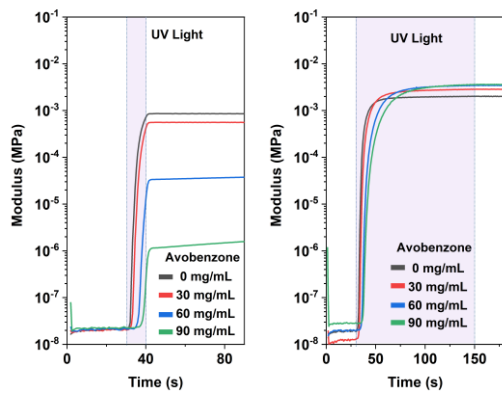


Figure S12. Photorheology curves of hydrogel with Avobenzone nanoparticles (0 - 90 mg/mL) during short (10 s) and long (120 s) duration light exposures (purple shaded region).

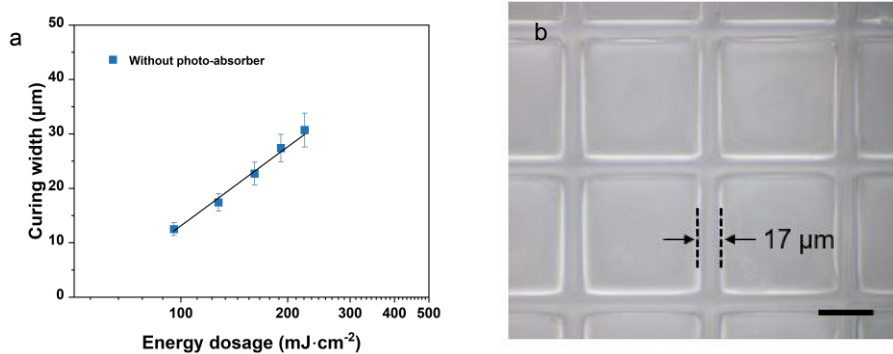


Figure S13. (a) Energy dosage on curing width without photo-absorber (light source: 405 nm). (b) 3D-printed hydrogel grid (30 wt.% PAAm hydrogel without photo-absorber, light source: 405 nm,  $63.8\ \text{mW}/\text{cm}^2$ , 2s). Scale bar:  $50\ \mu\text{m}$ .

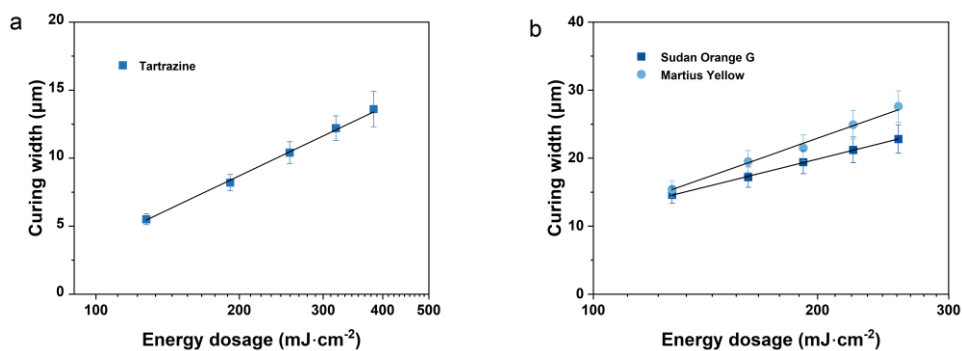


Figure S14. (a) Energy dosage on curing width with photo-absorber tartrazine (light source: 405 nm). (b) Energy dosage on curing width photo-absorber Sudan Orange G and Martius Yellow (light source: 405 nm).

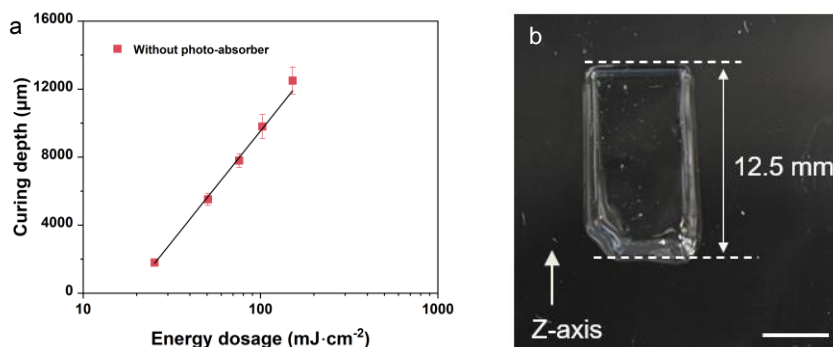


Figure S15. (a) Energy dosage on curing depth without photo-absorber (light source: 405 nm). (b) Curing depth of hydrogel under  $50.6\ \text{mW}/\text{cm}^2$  405nm light source for 3 s (20 wt.% PAAm hydrogel without photo-absorber). Scale bar:  $5\ \text{mm}$ .

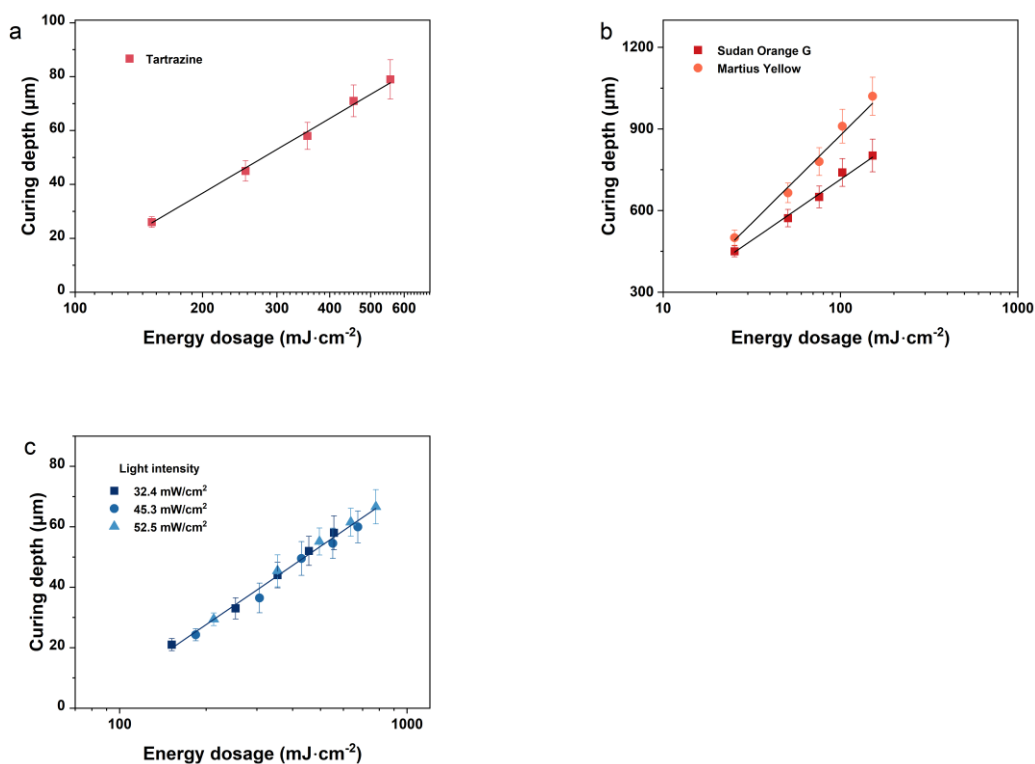


Figure S16. (a) Energy dosage on curing depth with photo-absorber tartrazine (light source: 405 nm). (b) Energy dosage on curing depth with photo-absorber Sudan Orange G and Martius Yellow (light source: 405 nm). (c) Energy dosage on curing depth under different light intensities (light source: 405 nm; photo-absorber nanoparticles: Sudan Orange G).

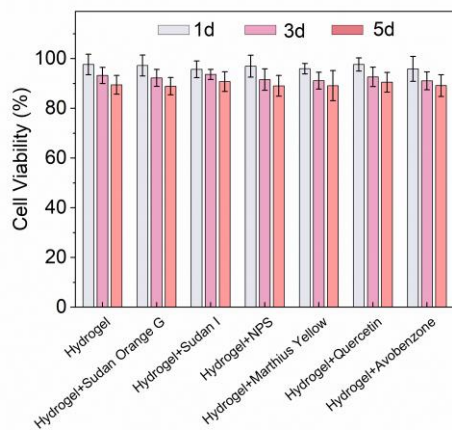


Figure S17. Live/dead assay for NIH 3T3 cells with hydrogels of different photo-absorber nanoparticles after 1d, 3d, and 5d.

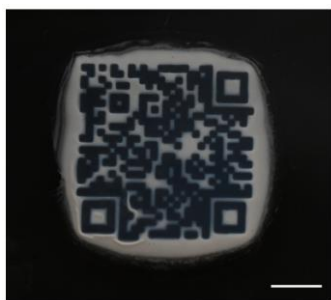


Figure S18. The photos of printed PNIPAAm hydrogel QR code without photo-absorber in hot water. Scale bar: 5 mm.



Table S1. Composition [% (w/w)] of the microemulsions before freeze-drying.

	<b>Photo-absorber</b>	<b>Ethyl acetate</b>	<b>Ethanol</b>	<b>SDS</b>	<b>PVP</b>	<b>H<sub>2</sub>O</b>
<b>Martius yellow</b>	1.7	22.3	21.0	7.5	7.5	40.0
<b>Sudan orange G</b>	1.7	22.3	21.0	7.5	7.5	40.0
<b>Avobenzone</b>	1.7	22.3	21.0	7.5	7.5	40.0
<b>Quercetin</b>	1.7	22.3	21.0	7.5	7.5	40.0
<b>NPS</b>	1.7	22.3	21.0	7.5	7.5	40.0
<b>Sudan I</b>	1.7	22.3	21.0	7.5	7.5	40.0

Table S2. Composition [% (w/w)] of the microemulsions before freeze-drying.

	<b>Photo-absorber (Sudan orange G)</b>	<b>Ethyl acetate</b>	<b>Ethanol</b>	<b>SDS</b>	<b>PVP</b>	<b>H<sub>2</sub>O</b>
<b>1</b>	0.8	23.2	21.0	7.5	7.5	40.0
<b>2</b>	1.7	22.3	21.0	7.5	7.5	40.0
<b>3</b>	2.6	21.4	21.0	7.5	7.5	40.0
<b>4</b>	3.8	20.2	21.0	7.5	7.5	40.0
<b>5</b>	5.0	19.0	21.0	7.5	7.5	40.0
<b>6</b>	6.5	17.5	21.0	7.5	7.5	40.0
<b>7</b>	8.1	15.9	21.0	7.5	7.5	40.0
<b>8</b>	10.0	14.0	21.0	7.5	7.5	40.0

Table S3. Load ratio [% (w/w)] of the photo-absorber in the freeze-dried powders.

<b>Photo-absorbers</b>	<b>W<sub>PA</sub></b>	<b>Theoretical <i>LR</i></b>	<b>Effective <i>LR</i></b>
<b>Marthius Yellow</b>	1.7	10	2.2
<b>Sudan Orange G</b>	1.7	10	4.9
<b>Avobenzone</b>	1.7	10	1.6
<b>Quercetin</b>	1.7	10	8.3
<b>NPS</b>	1.7	10	3.1
<b>Sudan I</b>	1.7	10	3.6

Table S4. Load ratio [% (w/w)] of the photo-absorber (Sudan orange G) in the freeze-dried powders.

	<b>W<sub>PA</sub> (Sudan orange G)</b>	<b>Theoretical <i>LR</i></b>	<b>Effective <i>LR</i></b>
<b>1</b>	0.8	5	3.0
<b>2</b>	1.7	10	4.9
<b>3</b>	2.6	15	7.4
<b>4</b>	3.8	20	9.6
<b>5</b>	5.0	25	13.0
<b>6</b>	6.5	30	14.5
<b>7</b>	8.1	35	17.9
<b>8</b>	10.0	40	17.9